

## Tunable multiple-scattering system

John A. Scales and Kasper Van Wijk<sup>a)</sup>

*Physical Acoustics Laboratory and Center for Wave Phenomena, Department of Geophysics, Colorado School of Mines, Golden, Colorado 80401*

(Received 13 March 2001; accepted for publication 13 July 2001)

To study the propagation of multiply scattered waves, it is useful to have a medium in which the scattering properties can be easily controlled. Here, we describe such a system; it involves the propagation of ultrasonic surface waves in a medium with an aligned, disordered pattern of grooves. Waves propagating parallel to the grooves see a homogeneous medium; waves propagating perpendicular to the grooves are strongly scattered. By varying the source–receiver distance and orientation with respect to the grooves, we are able to map out the transition from ballistic to diffusive propagation. In addition, by using an optical detection system we are able to measure the wave motion *inside* the scattering medium. We measure the angle-dependent macroscopic properties of the medium, such as the group velocity as well as the mean-free path and the diffusion constant in the strong-scattering regime. © 2001 American Institute of Physics. [DOI: 10.1063/1.1402156]

The past ten years have seen a tremendous growth of interest within the physics community in understanding and exploiting multiply scattered waves. Recent work in medical imaging,<sup>1</sup> ultrasonics,<sup>2</sup> and seismology,<sup>3,4</sup> for example, has shown that multiply scattered waves exhibit extraordinary stability,<sup>5</sup> in spite of the complexity of the wave fields, and can be exploited in a variety of ways to provide information about the scattering medium.

The influence of multiple scattering in wave propagation measurements can be seen in many ways. There are subtle, long-wavelength effects such as anisotropy (if the scatterers are aligned) and attenuation (as energy is shifted from the ballistic pulse into the multiple-scattering coda).<sup>6</sup> However, in most cases the same experiment can be looked at from different points of view depending on the wavelength of the probing beam relative to the size of the disorder and on the distance propagated; for example, ballistic propagation, diffusion, or radiative transfer. To understand these different regimes, it would be extremely useful to have a medium in which the scattering properties could be easily adjusted. For example, with phonon scattering one can control the mean-free path via the temperature.<sup>7</sup> If the mean-free path is greater or equal to the size of the sample, then the phonons propagate ballistically. The more scattering between source and detector, the more diffusive the propagation. In Ref. 8, the authors use path-length resolution to separate light propagating in a highly scattering system into components based on the degree of scattering.

We describe a simple laboratory model to study multiple scattering of ultrasonic surface waves. We are able to parametrically vary the strength of the scattering so that we can continuously and reproducibly change the material properties from no scattering to strong multiple scattering. The model consists of a block of aluminum with 144 grooves in the pattern of a Fibonacci sequence etched into one face using a computer-controlled milling machine (Fig. 1). An angle-beam transducer launches plane surface waves into this disordered medium and a laser-Doppler vibrometer measures

the vertical component of the particle velocity on the surface. This setup allows us to measure multiply scattered waves *inside* the scattering medium. The grooves are 1 mm wide by 3 mm deep and the dominant wavelength of the surface waves is about 15 mm, so there are many scatterers per wavelength when the waves are propagating perpendicular to the grooves. [See Scales and Van Wijk<sup>9</sup> (SVW), for more details on the model.]

SVW showed measurements of propagation parallel and perpendicular to the grooves. For propagation parallel to the grooves the surface wave propagated attenuation and dispersion free, whereas for propagation perpendicular to the grooves there was strong multiple scattering, causing long-wavelength anisotropy and apparent attenuation. Here, we extend these results to include the complete angle-dependent behavior of the scattering. We use the angle of propagation as a parameter to tune the scattering properties of the medium. We measure the angle-dependent group velocity. We also describe how the multiple-scattering coda can be used to estimate both microscopic scattering properties such as the mean-free path, and macroscopic material parameters such as the effective diffusion constant and attenuation.

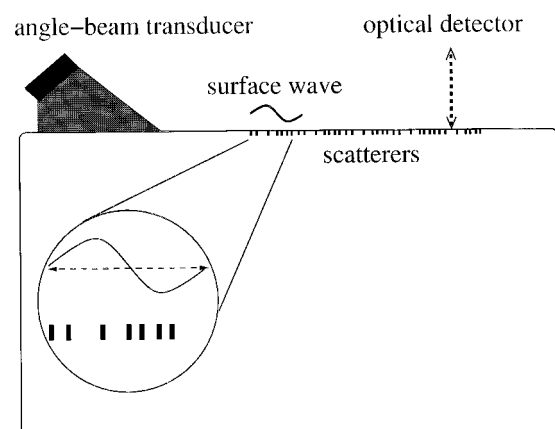


FIG. 1. The angle-beam transducer launches nearly plane surface waves of dominant wavelength 15 mm into the grooved aluminum block. The grooves are 3 mm deep and 1 mm wide.

<sup>a)</sup>Electronic address: kasper@acoustics.mines.edu

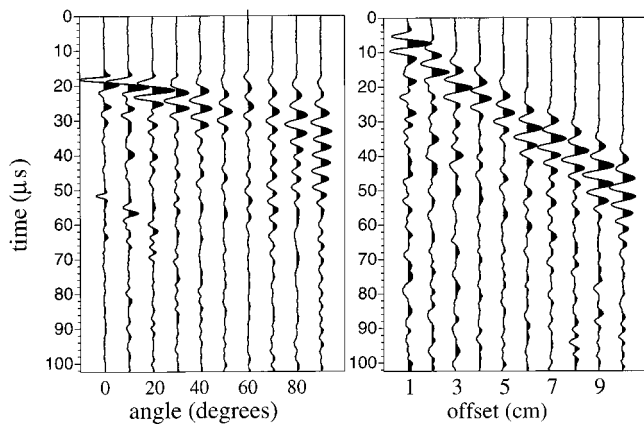


FIG. 2. On the right is a constant-angle section (50°); that is, variable source–receiver distance at a fixed angle relative to the grooves. On the left is a constant-offset section (5 cm offset); that is, variable angles for a fixed source–receiver distance.

The experimental setup is described in SVW. The basic measurement that we make consists of the vertical component of particle velocity measured at 1 cm increments, or *offsets*, along a line extending perpendicularly from the transducer front to a maximum offset of 10 cm. We refer to such a measurement as a *constant-angle section*. The line along which the measurements are made defines an angle relative to the orientation of the grooves. We recorded constant-angle sections from 0° to 90°, with 10° spacing; thus, there are a total of 100 traces (10 angles and 10 offsets).

Figure 2 shows a subset of the data. As shown in SVW, 0° propagation is essentially identical to propagation on the smooth surface of aluminum, which is attenuation and dispersion free. However, as the angle of the propagation increases, scattering becomes significant. In the constant-offset section we see a transition from ballistic propagation to strong multiple scattering as the angle is increased.

In the absence of scattering, the dominant frequency is around 250 kHz. However, scattering reduces the high-frequency power in the data, because the 3-mm-deep grooves scatter the shallower-traveling high frequencies more effectively. Figure 3 shows the power spectrum at four different angles computed for 5 cm constant-offset data.

The longer effective path lengths of the multiply scattered waves result in a significant slowing down of the energy propagation. To estimate this group or energy velocity as a function of angle, we sorted the data into constant-angle

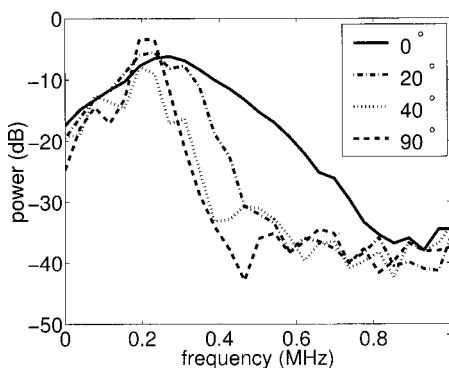


FIG. 3. Power spectra of the 5 cm offset data for four propagation angles relative to the grooves.

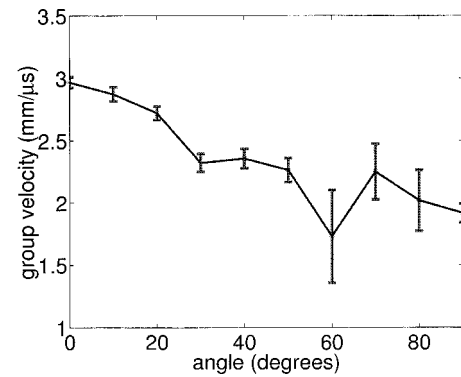


FIG. 4. Group velocity decreases as the scattering strength increases as energy is shifted into the coda.

sections and computed the energy envelopes of each trace. The peaks of these envelopes were picked automatically and the times taken to be the arrival times of the pulse. This gives an arrival time for each offset, the set of which were fit with a straight line to arrive at the group velocity (Fig. 4). The error bars are 98% coverage intervals from the regression. Destructive interference causes intensities from 60° to 80° to be lower, making the error bars in the group velocity estimate larger.

Even though it is not a truly random medium, we can exploit the spatial disorder of the Fibonacci grooves<sup>10</sup> to estimate the scattering mean-free path of the medium as well as study the transport of energy. Figure 5 shows traces recorded at a fixed offset of 5 cm, for 38 different positions in the medium. The location of the fixed source/receiver pair was incremented between shots by 2 mm along the source/receiver axis, perpendicular to the grooves. These traces have been corrected for minor positioning errors by aligning the traces via cross correlation.

Let  $u(\mathbf{r}_i, t)$  denote one of 38 realizations of the measured field  $u$  (particle velocity). We will treat the different traces as 38 realizations of a time-varying random process  $u(\mathbf{r}, t)$ . We use angle brackets  $\langle \cdot \rangle$  to denote expectation with respect to this random process. The coherent field is then  $\langle u \rangle$ . The total field can be expressed  $u = \langle u \rangle + u_f$ , where  $u_f$  is the fluctuating part of the field. All intensities are ensemble averaged intensities. The total intensity  $I_t$  is the intensity of the total field:  $I_t = \langle |u|^2 \rangle$ . The coherent intensity is  $I_c = |\langle u \rangle|^2$ . For a plane wave normally incident in a semi-infinite medium filled with random scatterers, the total and coherent intensities are expected to decay exponentially as

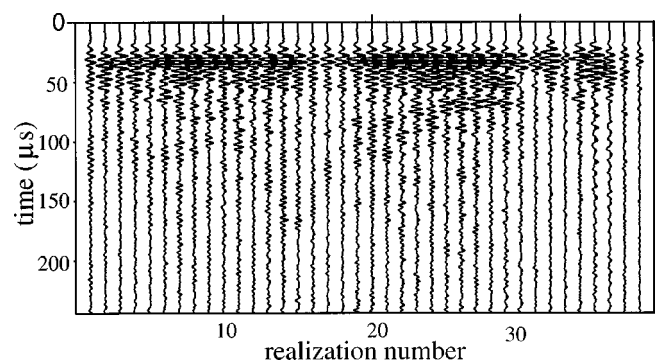


FIG. 5. 38 traces recorded at a fixed offset of 5 cm on the block. The source/receiver combination was offset by 2 mm between shots.

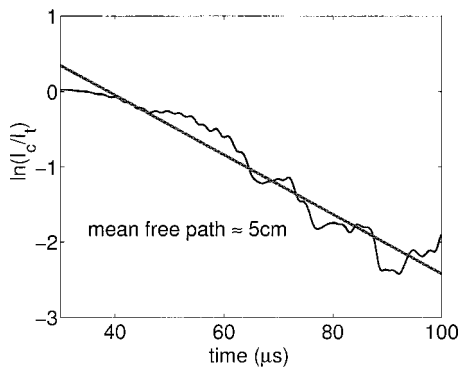


FIG. 6. Ratio of coherent to total intensities averaged over the ensemble of realizations. The curve decays after the coherent arrival. This decay is fit with an exponential, the decay constant of which is the mean-free time; in this case,  $24 \mu\text{s}$ .

(see Ref. 11, Sec. 14-3):  $I_t(x) = I_0 \exp(-x/l_a)$  and  $I_c(x) = I_0 \exp(-x/l_a) \exp(-x/l_s)$ , where  $l_a$  and  $l_s$  are the absorption and scattering mean-free paths, respectively. Therefore, the ratio of these two intensities depends only on the scattering mean-free path:<sup>12</sup>

$$\frac{I_c(x)}{I_t(x)} = \exp(-x/l_s) = \exp(-vt/l_s) = \exp(-t/\tau_s),$$

where  $v$  is the energy velocity and  $\tau_s$  is the scattering mean-free time.

To apply this result, we compute the coherent and total intensities; numerically,  $I_c$  is just the intensity of the average trace, while  $I_t$  is the average of the intensities of the individual traces. The ratio of  $I_c$  to  $I_t$  is shown in Fig. 6. By fitting an exponential to the portion of the curve after the coherent arrival (about  $30 \mu\text{s}$ ), we get a mean-free time  $\tau_s = 24 \mu\text{s}$ . Since this measurement is for propagation at  $90^\circ$  with respect to the grooves, the group velocity is around  $2 \text{ mm}/\mu\text{s}$ , which gives a mean-free path of just under  $5 \text{ cm}$ . Thus, we are in a regime in which the wavelength is large compared to the size of an individual scatterer, but small compared to the mean-free path; while we have measurements with source–receiver offsets as large as two mean-free paths. In this sense we can see the transition from ballistic to diffusive propagation, even though, strictly speaking, there is no such thing as diffusion in a one-dimensional (1D) random medium, since any random disorder is localizing.<sup>13</sup>

To see whether the measured waves behave diffusively at  $5 \text{ cm}$  offset, as suggested by our estimate of the mean-free path, we fit the ensemble-averaged total intensities with an analytic model associated with propagation in a homogeneous diffusive, absorbing medium. (We included an absorbing term in order to account for diffractive losses off the bottom of the grooves.) The Green's function for this model is given by

$$I(x,t) = (4\pi Dt)^{-1/2} \exp\left(-\frac{x^2}{4Dt} - D\kappa^2 t\right),$$

where  $\kappa = 1/l_a$  is the absorption coefficient,  $D$  is the diffusion constant, and  $x$  is the propagation distance. The fit is shown in Fig. 7. This fitting alone cannot determine  $D$ , explicitly; the propagation distance is not well defined since in the real experiment the waves propagate ballistically for

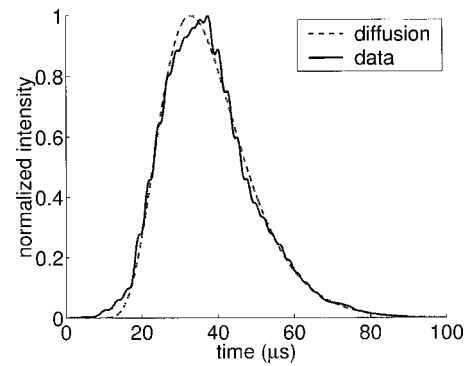


FIG. 7. Fit of intensity to a model involving propagation in a 1D diffusive, attenuative medium. The attenuation is an approximation to diffractive losses off the bottom of the grooves.

some distance, whereas the model is for a homogeneous diffusive medium. However, we can get a rough estimate of the diffusion constant as follows. First,  $D = v l_{tr}/d$  where  $v$  is the transport velocity,  $l_{tr}$  is the transport mean-free path, and  $d$  the dimension of the experiment. Our method of measuring the energy envelope yields the group velocity for weak scattering, but for strong scattering the energy propagates according to the transport velocity. So, for  $90^\circ$  propagation  $v \approx 2 \text{ mm}/\mu\text{s}$ . If in the strong scattering regime where the ensemble of wave forms was measured, the transport mean-free path is equal to the scattering mean-free path, the diffusion constant is  $2 \times 50/2 \text{ mm}^2/\mu\text{s}$  in two dimensions. We are in the process of extending our measurements of distance dependence of the intensity, which should allow us to estimate  $D$  independently. This will also ensure that the estimated scattering mean-free path is not an artifact of the source–receiver distance.

We acknowledge stimulating discussions with Roel Snieder of CSM and Philippe Roux and Julien De Rosny of the Laboratoire Ondes et Acoustique, École Supérieure de Physique et de Chimie Industrielles de la Ville de Paris. This work was begun while one of the authors (J.S.) was on sabbatical in the ESPCI. J.S. wishes to express his gratitude to his colleagues in Paris for their hospitality. This work was partially supported by the U.S. Army Research Office under Grant No. DAAG55-98-1-0070, by the sponsors of the Consortium Project on Seismic Inverse Methods for Complex Structures at the Center for Wave Phenomena, The French Academy of Sciences, and Total Fina Elf.

- <sup>1</sup>D. Boas, L. Campbell, and A. Yodh, *Phys. Rev. Lett.* **75**, 1855 (1995).
- <sup>2</sup>A. Derode, P. Roux, and M. Fink, *Phys. Rev. Lett.* **75**, 4206 (1995).
- <sup>3</sup>R. Snieder, in *Diffuse Waves in Complex Media*, edited by J.-P. Fouque (Kluwer, Amsterdam, 1999), p. 405.
- <sup>4</sup>R. Hennino, N. Trégourès, N. M. Shapiro, L. Margerin, M. Campillo, B. A. Van Tiggelen, and R. L. Weaver, *Phys. Rev. Lett.* **86**, 3447 (2001).
- <sup>5</sup>J. Scales and R. Snieder, *Nature (London)* **401**, 739 (1999).
- <sup>6</sup>J. Groenenboom and R. Snieder, *J. Acoust. Soc. Am.* **98**, 3482 (1995).
- <sup>7</sup>J. Wolfe, *Imaging Phonons: Acoustic Wave Propagation in Solids* (Cambridge University Press, Cambridge, 1998).
- <sup>8</sup>K. Bizheva, A. Siegel, and D. Boas, *Phys. Rev. E* **58**, 7664 (1998).
- <sup>9</sup>J. Scales and K. Van Wijk, *Appl. Phys. Lett.* **74**, 3899 (1999).
- <sup>10</sup>P. Carpena, V. Gasparian, and M. Ortuno, *Phys. Rev. B* **51**, 12813 (1995).
- <sup>11</sup>A. Ishimaru, *Wave Propagation and Scattering in Random Media* (Oxford University Press, Oxford, 1997).
- <sup>12</sup>J. D. Rosny and P. Roux, *J. Acoust. Soc. Am.* **109**, 2587 (2001).
- <sup>13</sup>J. Scales and E. Van Vleck, *J. Comput. Phys.* **133**, 27 (1997).